Structuring and characterization of a novel highly microporous PEI/BMI semi-interpenetrating polymer network ☆

Jamal Kurdi, Ashwani Kumar*

Institute for Chemical Process and Environmental Technology, National Research Council of Canada, Montreal Road Campus, Ottawa, Ont., Canada K1A 0R6

Abstract

Syntheses of semi-interpenetrating polymer networks (semi-IPNs) with polyetherimide/bismaleimide (PEI/BMI) chromophore composites showing molecular sieve characteristics are reported. A tunable and compatible chemical structure with fine morphology was obtained through in situ controlled sol–gel polymerization, crosslinking, chemical modification and membrane fabrication. The novel semi-IPN synthesized and assembled using ethanol as polar protic modifier and pore former, had superior structure and morphology for making gas separation membranes. These semi-IPN membranes gave 15 times higher gas flux than those membranes prepared from pure PEI without significant decrease in gas selectivity. The chemical structures of these novel semi-IPNs were elucidated by FTIR, XPS and SEM. It appears that in situ simultaneous ethoxylation, anionic polymerization of BMI and imide modifications were responsible for creating the new chemical structure and molecular morphology that was different from traditional BMI resins. In addition, these chemical processes give superior structures using green chemistry techniques such as ambient temperature reaction and polymerization without initiators.
Crown Copyright © 2005 Published by Elsevier Ltd. All rights reserved.

Keywords: Semi-IPN; BMI; PEI

1. Introduction

Most commercial asymmetric membranes are fabricated from engineering plastics using different techniques to obtain ultra thin skin layer and high microporosity for improved productivity. However, achieving ultra thin skin layer in itself is not sufficient to increase the membrane productivity and researchers have explored a mixed matrix polymeric network to increase the microporosity of membrane materials [1]. The need for material improvement and development has been emphasized by leading scientists [2]. Incorporation of one or more different components (organic or inorganic) into a polymeric material to increase the microporosity suffers from many obstacles such as creation of defects particularly in ultra thin films, incompatibility among different phases and the lower stability. Therefore, it is still a challenge to form a highly

microporous polymeric network that is free of defects and has higher stability than the base polymer. Formation of interpenetrating polymer network (IPN) could be one of the most important ways for material development as indicated in vast engineering literature, patents and commercialized products reported since 1951 [3]. Using in situ polymerization and appropriate processing led to a revolutionary success in creating polymeric nano-scale multidomain blends having new extraordinary properties as reviewed elsewhere [4,5]. It was reported that gas transport characteristics correlated with the chemical structure and matrix morphology, might be tailored by controlling the conditions of IPN formation as illustrated elsewhere [6]. However, these polyurethane–polystyrene IPNs were not used to prepare commercial gas separation membranes.

As a class of IPN semi-interpenetrating polymer networks (semi-IPNs) were also recognized not only to tune composite material properties but also to control material morphology with a desirable balance between homogenous and heterogeneous structures [7] required in gas separation membranes. For example, BMI/polysulfone semi-IPN was

prepared from *N*-methylpyrrolidone casting solution and anionic initiator. However, the morphology of the cured films examined by optical microscopy (magnification 1200 times) showed a phase separation [8]. This undesirable phase separation might be attributed to heating the stagnant cast film at curing temperatures that were higher than glass transition temperature of PSF before and during polymerization of BMI as illustrated elsewhere [9,10]. On the other hand, it was reported that a homogenous semi-IPN could be achieved by mixing BMI oligomer/polyimide in a rotary roller for 24 h within a highly viscous NMP/polyimide solution. BMI oligomers act as a plasticizer for polyimides that led to the formation of semi-IPNs containing microphase domains that were smaller than 0.25 μm, which is beyond the resolution limit of optical polarized microscopy [11]. However, this work was aimed to prepare semi-IPNs suitable for microelectronic industry and was not used to prepare gas separation membranes. In a more relevant patent, formation of semi IPN type polymer alloy and fabrication of asymmetric membranes has been described [12]. The procedure involved curing at ambient temperature in the presence of a photoinitiator and ultraviolet ray to make hydrophilic ultrafiltration membranes. However, one major disadvantageous of these membranes was that a very small flux was obtained for a low molecular weight cut-off membrane. Therefore, their route of IPN synthesis might not be suitable to prepare highly microporous gas separation membranes. In their method, polymerization of vinyl monomers was carried out inside a stagnant film of a thermoplastic polymeric solution, which might lead to formation of a gel within the polymeric solution before water coagulation and membrane formation. Termination of polymerizing vinyl monomers to control the size of growing microphase at different polymerization stages was not considered in their method and enhancement of component dispersion by mixing was not used. It is possible that structuring and enhancing the dispersion of the thermoset/thermoplastic semi-IPNs and termination of monomer polymerization at a controlled stage might be combined with appropriate membrane formation to produce a highly permeable and homogeneous structure that would be suitable for gas separation membranes. This work reports a green chemistry approach for the fabrication of novel PEI/BMI semi-IPNs asymmetric membranes and their gas transport characteristics.

2. Experimental

2.1. Materials

Aromatic polyetherimide (PEI) Ultem® 1000, was supplied by General Electric Plastics, USA in pellet form and was dried in an oven at 150 °C for 8 h before use. Anhydrous 1-methyl-2-pyrrolidinone (NMP), Aldrich, 99.5%, reagent grade, (water < 0.005%), anhydrous isopropanol

99.5% and 1,1′-(methylenedi-4,1-phenylene) bismaleimide (BMI) 95% were supplied by Sigma-Aldrich Canada Ltd. Chemical structures of PEI, BMI and NMP are given in Table 1. Anhydrous ethyl alcohol was received from Commercial Alcohols Inc., Ont., Canada. Hexanes of ACS reagent grade were supplied by VWR, Canada. All solvents were used as supplied under a dry nitrogen atmosphere. Ultra high purity helium and medical air were supplied by BOC Gases Canada Ltd and used as received without further purification.
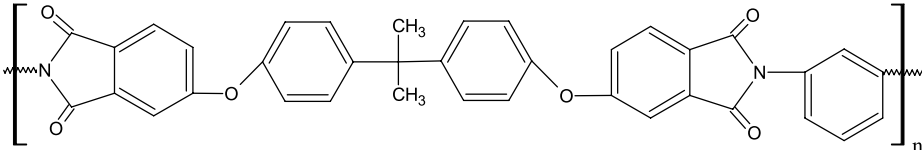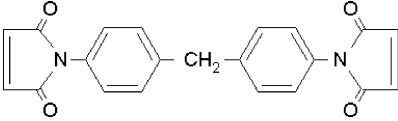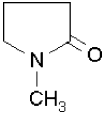
2.2. Membrane preparation

Samples of polyetherimide (PEI) with and without 1,1′-(methylenedi-4,1-phenylene) bismaleimide (BMI) were prepared as flat asymmetric membranes by sol–gel technique [13]. Polymerization of BMI monomer was carried out in polymeric solutions containing anhydrous 1-methyl-2-pyrrolidinone (NMP) as an aprotic dipolar solvent and one of the non-solvents, anhydrous ethyl alcohol (EtOH) or isopropyl alcohol (i-PrOH). The PEI was selected because it provides a hydrophobic shield [14] and acts as an ion stabilizer, i.e. as a catalyst for an electron transfer shuttle process [15]. The two protic non-solvents were selected because they act as diluents for forming the porous structure [16] and as a proton donor to enhance BMI polymerization. In addition to these criteria, i-PrOH and EtOH have different polarity and dielectric constant that may influence BMI polymerization process to a varying degree. The ratio (w/w) of BMI to PEI was selected to be 11% because a higher value led to a brittle polymer network. The weight percent of the non-solvent was kept at one-fifth of NMP weight so that the final solution was close to its clouding point [17]. Based on these criteria four different polymer solutions with compositions shown in Table 2 were prepared by mixing PEI and BMI in NMP. After PEI and BMI were completely dissolved, the non-solvent was mixed in this solution. Mixing of these solutions was continued under normal light for 30, 60 and 80 days.

To prepare membrane films, homogenous solutions with compositions shown in Table 2 were cast at room temperature on clean glass plates placed in a glove box equipped with a gas filter. After casting each sample with a doctor knife having a gap of 250 μm, the plate was quickly immersed in distilled water at ambient temperature. The membrane films were left in water for 3 days then washed and stored in an anhydrous EtOH bath for 1 day. Membranes were subsequently placed in hexanes for 1 day before leaving them in a fume hood for 1 day. Drying was carried out at 80 °C in air-purging convection oven for 1 day and finally in vacuum oven at 80 °C and 725 mmHg vacuum pressure for 2 days. Three circular coupons of 7.4 cm diameter were cut from each sample to be used in the permeation test while other pieces were cut from the same cast membrane for characterization.

Membranes used in the permeation test were coated with silicon rubber. A solution of 3% Sylgard-184 (with a

Table 1
Chemical structure of PEI, BMI and NMP

Component	Chemical structure
PEI	
BMI	
NMP	

catalyst to base rubber ratio of 1:10) in *n*-pentane was sprayed as a thin layer on the top surface of the membrane and the solvent was allowed to evaporate. Application of four coatings was found to be adequate for making a gas separation membrane. Finally, the coated silicon rubber was cured in air purging convection oven at 80 °C for 1 day.

2.3. Chemical structure analysis

Membrane samples without silicon rubber coating were examined by scanning electron microscopy (SEM) using JEOL 840A equipment at an accelerating voltage of 10 kV. Samples were prepared by cutting a strip from membrane, freezing in liquid nitrogen and fracturing to obtain a representative sample. They were mounted on carbon tape on 45° SEM stubs and sputter coated with gold. Photographs were taken at a magnification of 5000.

Fourier transform infrared attenuated total reflection (FTIR-ATR) analysis was performed using a SuperCharged ZnSe single-bounce ATR crystal with a tensor FTIR spectrometer (Bruker IFS 66). The spectra were taken with 200 scans at a resolution of 4 cm^{-1} in the range 400–4000 cm^{-1}. For X-ray photoelectron spectroscopy (XPS) experiments, each sample was mounted on a piece of conductive carbon tape. The samples were analyzed, as received, using the Kratos AXIS Ultra XPS (X-ray photoelectron spectroscopy) equipped with a hemispherical analyzer, a DLD (delay line detector), charge neutralizer and a monochromatic Al K$_\alpha$ X-ray source. Analyses were

performed using an accelerating voltage of 14 kV and a current of 10 mA. Survey scans were performed at a pass-energy of 160 eV. Species detected by survey scan were then analyzed at a pass-energy of 40 eV and quantified. The FTIR and XPS experiments were carried out on all membrane samples before coating with silicon rubber.

2.4. Permeation test

A cross-flow test cell having a permeation surface area of 9.6 cm^2 was used. Medical air was used at feed pressure of 665 kPa guage (498.8 cmHg) and the retentate was set at a flow rate of 6.6 ml (STP) s^{-1} while the permeate was discharged to atmosphere. The permeate flow rate was measured by a soap bubble flow meter while oxygen concentration of permeate was determined by gas chromatography.

3. Results and discussion

Preliminary experiments were performed to explore and set appropriate experimental procedures. It was found that BMI undergoes a slow reactive substitution and/or self-polymerization at ambient temperature in the presence of both light and a proton donor when it is incorporated into a dissolved glassy polymer having an electron acceptor group such as phthalimide or sulfone in dipolar aprotic solvent such as NMP. This chemical process does not need

Table 2
Compositions of polymeric solutions used in this study

Samples	Composition, percent (w/w) of the total solution				
	PEI	NMP	BMI	EtOH	i-PrOH
PEI–EtOH	19.5	67.2	0	13.3	0
PEI–i-PrOH	19.5	67.2	0	0	13.3
PEI–BMI–EtOH	17.6	67.2	1.9	13.3	0
PEI–BMI–i-PrOH	17.6	67.2	1.9	0	13.3

complicated initiators for polymerization and have the advantage of using green chemical components such as EtOH, i-PrOH, NMP, BMI and PEI. We observed that color and viscosity of these polymeric solutions changed after mixing for a long period of time, which indicated that BMI due to its reactivity might be involved in some kind of reactions. When EtOH is used as a proton donor, the color of the polymeric solution gradually changed from brown-yellow to a bright crimson color (bright bloody red color) accompanied with an increase in the observed viscosity of the solution. It took 30 days to notice the change in the color and approximately 60 days to reach its brightest color and then the solution starts to be cloudy, less transparent with a decrease in brightness and changed the color to a more brownish. Phase separation was clearly observed indicating the appearance of two polymer phases. The last phenomenon is well known in literature for the phase separation of thermoset/thermoplastic polymeric blends [18,19] and particularly for BMI/PEI blends [20]. This phase separation was also observed by scanning electron microscopy as shown in Figs. 1–3. It is clear that an increase in the size and number of cavities has taken place from Figs. 1–3 as the mixing time increases. The sizes of these approximately rounded cavities, which appear partially filled by another solid phase, exceed 1 μm for membrane cast after 80 days. Usually these membranes were not suitable for gas separations due to the presence of cavities and particularly for an ultra-thin skin asymmetric membrane as they are more prone to have these defects than thick flat films.

Similar observations were made when isopropanol was used as a proton donor instead of EtOH. However, the change in the color was from brown-yellow to a darker yellow. This indicates that a different composite structure was synthesized in the case of isopropanol. The red color of the polymeric solution was attributed to a carbanion when nanocrystalline titania was used as a catalyst to polymerize BMI as discussed elsewhere [21]. This color was also reported to indicate the occurrence of anionic
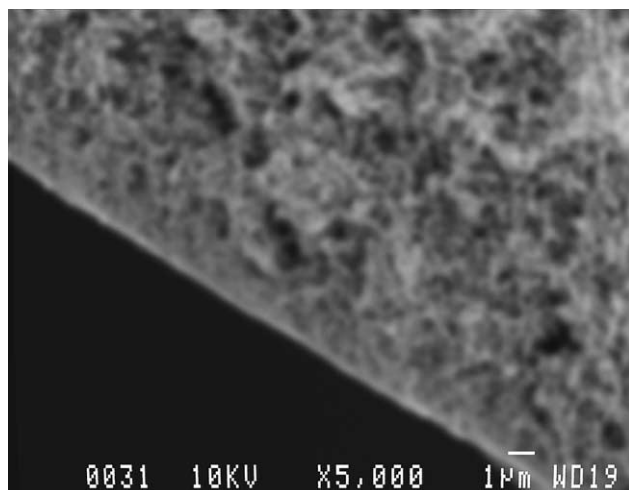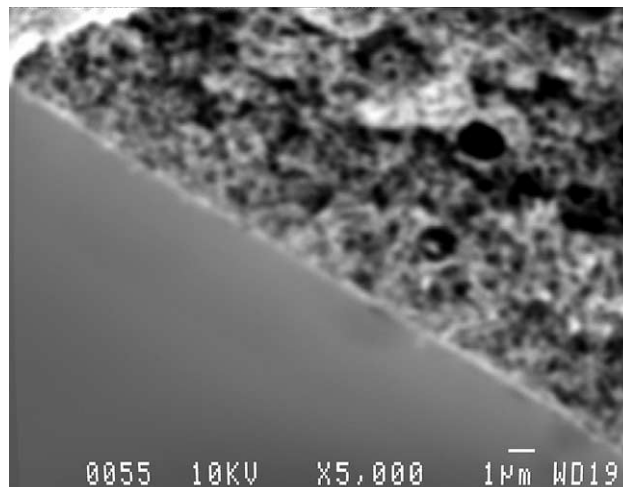

Fig. 2. Micrograph of PEI–BMI–EtOH membranes casted after 60 days obtained by SEM (×5000).

polymerization of BMI [22]. Absence of red color in the case of isopropanol indicates that BMI probably undergoes a free radical polymerization as reported elsewhere [23]. Additional experiments showed that the above process could be accelerated if temperature was increased to 50 °C or solution was irradiated with ultra-violet light. However, as the BMI polymerization process advanced slowly, it was possible to watch and control the thermoset phase size and separation in the semi-IPNs as a case study. Stopping the polymerization and phase separation processes at different periods of time could be achieved by polymer gellation through casting and membrane formation.

We also conducted similar experiments to polymerize BMI in the presence of proton donor and light but in the absence of PEI. After 80 days, we did not observe any change in the BMI solutions indicating that PEI has an important role as a catalyst in BMI polymerization. As a first explanation, we suggest that phthalimide groups in PEI acts
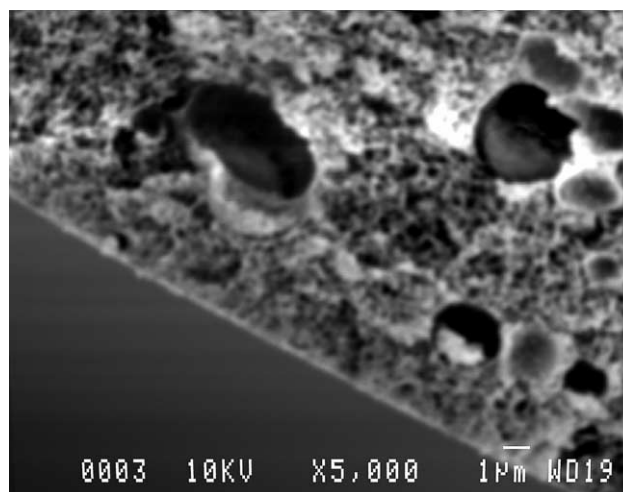

Fig. 1. Micrograph of PEI–EtOH membrane obtained by SEM (×5000).

Fig. 3. Micrograph of PEI–BMI–EtOH membranes casted after 80 days obtained by SEM (×5000).

as a polymerization catalyst because these groups are excitable by light. The role of PEI as a catalyst could be similar to the role of nanocrystalline titania in catalytic anionic polymerization of BMI. Additional experiments were conducted to polymerize BMI in PEI/NMP solutions but without ethanol as a proton donor. After 80 days, no red color was observed indicating that ethanol plays a vital role in anionic polymerization of BMI. However, characterization of the chemical structure of the gelled network resulted from polymerization of BMI in PEI solution might provide more information about this chemical process. It is worth noting that the novel semi-IPN membranes formed in this work showed an enhanced solvent resistance, as they are partially soluble in chloroform while PEI is completely soluble in chloroform.

3.1. Chemical structure analysis

3.1.1. FTIR analysis

Fourier transform infrared attenuated total reflection (FTIR-ATR) spectra for PEI–EtOH, PEI–BMI–EtOH-S, PEI–BMI–EtOH-L, and PEI–BMI–i-PrOH-S membranes in the range of 700–1900 cm^{-1} are shown in Fig. 4. The additional S and L symbols refer to solutions that were mixed for 30 and 60 days, respectively. Spectra for all membranes were adjusted to have the same base line and to pass through at wavelength 1850 cm^{-1} where no peak would be expected. Spectra were also normalized to an invariant reference peak at 1600 cm^{-1}, which might be assigned to aromatics found in both PEI and BMI with slightly different concentrations. This normalization was useful for qualitative comparison of various spectra.

The FTIR spectrum of membrane PEI–i-PrOH was

similar to that of PEI–EtOH while the spectrum for PEI–BMI–i-PrOH-S was similar to that of PEI–BMI–i-PrOH-L. Therefore, these spectra were deleted, as they did not provide any additional information. Comparing the FTIR spectrum of PEI–EtOH membrane with commercial Ultem 1000 [24], the same peaks were observed particularly in the fingerprint region (900–1300 cm^{-1}) as defined elsewhere [25]. As shown in Fig. 4, FTIR spectra of PEI–BMI–EtOH S and L were significantly different from those of PEI–EtOH or PEI–BMI–i-PrOH membranes. This might be attributed to significant changes in the structure of these membranes. Through data analysis, we have considered the influences of incorporation of BMI or possible complexation with some of the used solvents on the spectra, as each component has a different stoichiometric atomic concentration for each elemental chemical state as shown in Table 3. Assignments for FTIR peaks for contributions that were responsible for the differences between spectra of PEI–EtOH and PEI–BMI–EtOH membranes were summarized in Table 4. These peaks might also be representing other contributions as will be described in the following paragraphs.

The peak at 850 cm^{-1} labeled (a) was mainly assigned to C–H out-of-plane bending of *para*-substituted aromatic ring [26]. The small increase in the intensity of this peak in spectra of PEI–BMI–EtOH S and L might be attributed to the out of plane NH deformation as seen in Table 4 [27] that may result from the cleavage of the imide ring and formation of the amide group. It could possibly be attributed to the deformation of cyclobutane ring [28] that might form as a result of BMI polymerization [29]. These possibilities might be ruled out for PEI–BMI–i-PrOH as its spectrum showed a decrease in the intensity of this peak. A new peak at 881 cm^{-1} labeled (b) was observed in spectra of PEI–
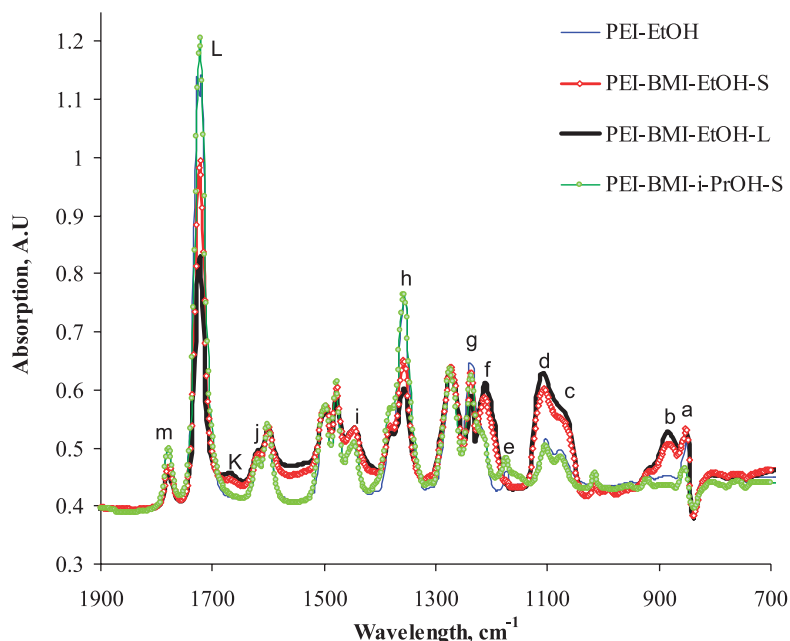

Fig. 4. FTIR spectra of polyetherimide-based membranes in the range 700–1900 cm^{-1}.

Table 3
Stoichiometric atomic concentration of different elemental chemical states for different components and their binding energies

Component	Formula	Total atoms	Theoretical atomic concentration (%)						
			Carbon				Oxygen		Nitrogen
			CC, CH	Ar C=C	CN, CO	OC=O, NC=O	carbonyl	Ether or OH	Imide
PEI	$C_{37}N_2O_6$	45	6.7	53.3	13.3	8.9	8.9	4.4	4.4
BMI	$C_{21}O_4N_2$	27	3.7	51.8	7.4	14.8	14.8	0	7.4
NMP	$C_5O_1N_1$	7	28.6	0	28.6	14.3	14.3	0	14.3
i-PrOH	C_3O_1	4	50	0	25.0	0	0	25.0	0
EtOH	C_2O_1	3	33.3	0	33.3	0	0	33.3	0
Binding energy (eV)			285	285	286.2	288.7	532	533.6	400.6

BMI–EtOH S and L which could be attributed to ethoxy group as illustrated elsewhere (Table 4) [30]. This peak (b) might also be attributed to O=C–O or O=C–N in amide group [31]. Due to the absence of this peak in PEI–EtOH spectrum, it appears that BMI has a major role in the ethoxy substitution, which probably occurred with the maleimide group in addition to the formation of amic acid (amide + carboxylic acid) resulting from imide cleavage. This simultaneous ethoxylation and imide cleavage might be supported through the well-known oxa-Michael ethoxylation process, which was illustrated and reported elsewhere [32]. The intensity of this peak was higher for PEI–BMI–EtOH-L than that for PEI–BMI–EtOH-S, which might be attributed to an increase in reaction time.

A significant increase was also observed in the intensity of two neighboring peaks in the spectra of PEI–BMI–EtOH (S and L). The peak at 1076 cm^{-1} labeled (c) was assigned to imide ring deformation [33] as well as to symmetric aryl ether [26] and the peak at 1105 cm^{-1} labeled (d) was assigned to p-phenylene CH in-plane bending [34]. According to del Arco and co-workers [35], the two peaks are formed upon dissociative adsorption of ethanol on acid–base sites of the MgAlW/500 solid. Around this wavelength

Table 4
Some FTIR contributions responsible for differences in spectra of PEI–EtOH and PEI–BMI–EtOH membranes

Wavelength (cm^{-1})		Assignment
PEI–BMI–EtOH	PEI–EtOH	
3268/3178	–	N–H stretch (amide)
–	1778	C=O symmetric stretch (imide)
–	1722	C=O asymmetric stretch (imide)
1670	–	C=O stretch (complexed NMP)
1618	–	C=O stretch (amic acid)
1446–1454	–	N–H and OH bend (amic acid) with H–bond
–	1357.7	C–N–C symmetric stretch (imide)
–	1240	Diarylether asymmetric stretch
1211	–	NH asymmetric bend (amide)
1105	–	C–O stretch (ethoxy group)
1076	–	C–C–O asymmetric stretch
881	–	C–C–O symmetric stretch
850	–	Out-of-plane NH deformation

range (1055 cm^{-1}), Cardenas and Acuna [36] observed the C–O stretching in primary saturated alcohol adsorbed on Ni. Therefore, the significant increase in these two peaks might be attributed to additional substituted ethoxy groups or/and existence of coordinated ethanol in the PEI–BMI–EtOH S and L membranes. This might also support the possibility of ethoxy presence as discussed above. A small decrease in the intensity of these two peaks for the spectra of PEI–BMI–i-PrOH was probably due to the absence of ether group in the structure of the incorporated BMI.

The peak at 1173 cm^{-1} labeled (e) could be mainly assigned to the CH symmetric bending of meta- and para-substituted aromatic rings [37] as well as asymmetric C–N–C stretching vibration mode [26,38]. The increase in the intensity of this peak for PEI–BMI–i-PrOH might be attributed to higher imide nitrogen in BMI than that in PEI as seen in Table 3. The formation of succinimide in this membrane might be possible as this peak could be assigned to C–N–C stretching in succinimide structure [4,38]. However, the decrease in the intensity of this peak in spectra of PEI–BMI–EtOH (S and L) might be attributed to imide cleavage. The shoulder peak at 1216 cm^{-1} labeled (f) and the peak at 1240 cm^{-1} labeled (g) were reported to be twin peaks [39] and could be assigned to asymmetric stretching in diarylether (Table 4) [26,40]. The peak (f) was observed to shift to a lower frequency (1211 cm^{-1}) with an increase in the intensity for PEI–BMI–EtOH (S and L) spectra. This might be attributed to additional contribution from the asymmetric C–N–C vibration mode of succinimide [41] or/and amide-out-of-plane N–H deformation [42]. Both possibilities could be resulting from BMI polymerization to form succinimide and imide cleavage to form amic acid. The intensity of peak (g) in PEI–EtOH spectrum was observed to decrease and shift to lower frequency (1236 cm^{-1}) in spectra of other membranes. As the major contribution was due to arylether without significant overlap by other type of structures, the decrease in the intensity of peak (g) might be attributed to the absence of ether group in the incorporated BMI.

The peak at 1357.7 cm^{-1} labeled (h) was assigned to C–N–C symmetric stretching [33] and CH$_3$ symmetrical bending umbrella mode in gem-dimethyl group [40]. The

decrease in the intensity of this peak might be attributed to opening of the imide ring especially for PEI–BMI–EtOH-L membranes. However, there was no significant difference in spectra of PEI–EtOH and PEI–BMI–i-PrOH membranes because incorporation of BMI led to an increase in atomic percentage of imide groups but a decrease in concentration of dimethyl groups.

The peak at 1446 cm^{-1} labeled (i) was assigned to the scissoring CH$_2$ symmetric bending [43] as well as to CH$_3$ asymmetric bending [40]. The increase in the intensity of the peak (i) with the appearance of a shoulder at 1454 cm^{-1} might be attributed to amide N–H bending [42] and OH bending [44] involved in hydrogen bonding (Table 4). Therefore, we might suggest the presence of amide in amic acid group in the structure of PEI–BMI–EtOH S and L membranes. The peak at 1618 cm^{-1} labeled (j) was assigned to aromatic C=C stretch [45] and the increase in this peak might be attributed to additional contribution from the carbonyl stretch in the amic acid [46]. The peak at 1670 cm^{-1} labeled (k) was assigned to the carbonyl stretch in a complexed NMP [11]. The presence of NMP in PEI–BMI–EtOH-L might indicate association with amic acid. This conclusion might be explained by the high affinity of NMP to form a complex with amic acid as illustrated elsewhere [37]. The peaks at 1722 cm^{-1} (L) and 1778 cm^{-1} labeled (m) were assigned to the asymmetric (out-of-plane) and the symmetric (in-plane) cyclic imide C=O stretching (Table 4) [11,37,40]. The decrease in these two peaks might be attributed to imide cleavage that led to the formation of amic acid. This possibility might also be supported by the presence of amic acid as indicated by other peaks in PEI–BMI–EtOH (S and L) spectra.

In the functional group region shown in Fig. 5, significant change was observed in two peaks at 3178 and 3268 cm^{-1}, which were higher for spectra of membrane containing BMI and particularly for PEI–BMI–EtOH (S and L) compared to PEI–EtOH. The increase in these two peaks might be attributed to NH stretching in amide group [4] (Table 4) resulting from hydrolysis and cleavage of imide groups, which have a higher concentration in BMI than PEI (Table 3). The remaining peaks were similar to the commercial PEI (Ultem 1000) film and had two major weak peaks at 2967.35 and 3067.21 cm^{-1} in addition to a very weak peak at 3521.9 cm^{-1} as described elsewhere [24].

3.1.2. XPS analysis

The X-ray photoelectron spectroscopy (XPS) provides useful information about the chemical composition of the surface of membrane materials. The XPS core-level spectra for PEI–EtOH, PEI–BMI–EtOH-S, PEI–BMI–i-PrOH-S, PEI–BMI–EtOH-L membranes were shown in Figs. 6–8 for elemental carbon, oxygen and nitrogen, respectively. The core-level spectra for PEI–i-PrOH and PEI–BMI–i-PrOH-L membranes were not shown as the first one was similar to PEI–EtOH membranes and the second to PEI–BMI–i-PrOH-S

with some insignificant differences. The spectral data for PEI (Ultem® 1000) film prepared from chloroform solution [47] were added in these figures for comparison. The linear baselines were set to the same value for all spectra in all figures. The charge correction of the binding energy scale for all actual experimental XPS data was achieved by shifting the total spectra for all elements by the same value in order to have the most intense peak for elemental carbon which was assigned in Table 3 at binding energy (BE) of 285 eV as described in literature [48]. The spectral data of PEI obtained from literature [47] was rescaled for comparison with the spectral data in this work. The total area of all peaks assigned for all elements in the XPS spectra of PEI was scaled to have the same total area as in the XPS spectra of PEI–EtOH membrane. We have also kept the percentage ratio for the areas of the elemental carbon, oxygen and nitrogen as in the reference source [47]. Therefore, these rescaled spectra can reproduce the same percentage atomic concentration of the assigned peaks exactly as in the source reference.

The core-level spectra of elemental carbon were shown in Fig. 6. Three types of carbon having binding energies with maximum located at 285, 286.2 and 288.7 eV were assigned as listed in Table 3 [47]. A fourth peak with maximum energy located at 291.4 eV was assigned to the shake up satellite of phenyl groups from π to π* [47]. The slight decrease in the first peak at 285 eV in spectrum of PEI–EtOH compared to PEI film dried from chloroform might be attributed to residual solvents. Additional decrease for the intensity of this peak might be attributed to incorporated components such as BMI, NMP, EtOH or/ and i-PrOH that contain a higher stoichiometric ratio of oxygen or nitrogen atoms to carbon atoms than that of PEI as seen in Table 3. These results could also be supported by the increase in the spectral intensity for binding energy between 286 and 287 eV where contribution from a relatively larger number of carbons having a single bond to nitrogen or/and oxygen is important [48]. An increase in the intensity of spectra of PEI–BMI–EtOH S and L might be attributed to the incorporation of a slight amount of NMP or/ and EtOH into the final composite structure that might be enhanced by the possible presence of amic acid moieties resulting from imide cleavage. The binding energy between 287.4 and 288.4 eV was assigned to carbonyl carbon in the amide moiety [49] and between 288.5 and 288.8 eV to carbonyl carbon in the imide moiety [49]. The increase in the intensity within the 287.4–288.4 eV range for the spectra of PEI–BMI–EtOH S and L might be attributed to the formation of the amide group resulting from the cleavage of the imide moiety that leads to formation of amic acid, which has greater ability than imide group for complexing with NMP, as discussed earlier. The binding energy peak between 288.8 and 289.5 eV was assigned to the carbonyl carbon in the carboxylic acid moiety [48]. The increase in the peak intensity in this range led to a shift in the imide peak from 288.6 to 288.8 eV, which indicated the
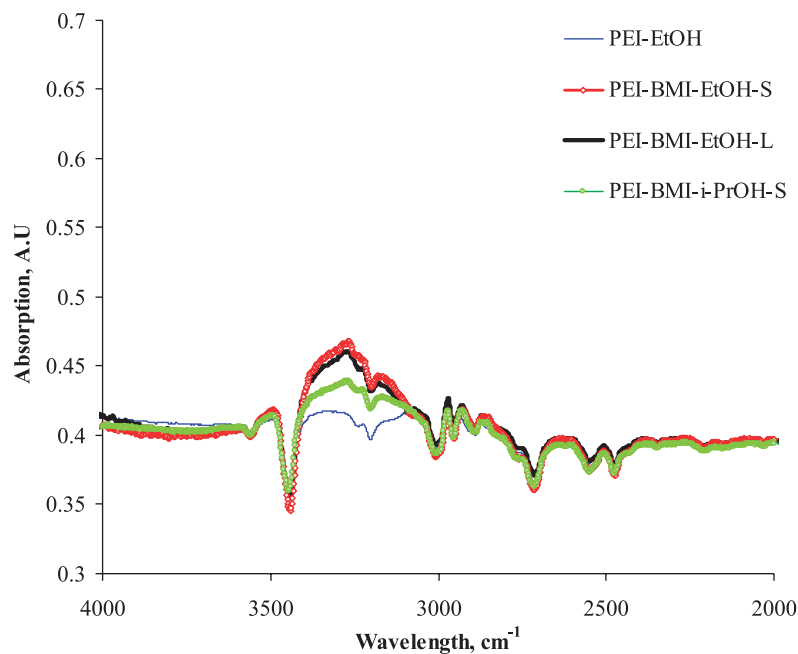
Fig. 5. FTIR functional group region spectra of polyetherimide-based membranes.

formation of a carboxylic group. Therefore, these results suggest the cleavage of the imide group and the formation of polyamic acid in PEI–BMI–EtOH S and L membranes. The decrease in the intensity of the weak broad peak between 290 and 294 eV assigned to the shake up satellite of phenyl groups from π to π^* [47] might indicate that the PEI–BMI–i-PrOH has a lower donor–acceptor charge transfer complexation compared to other membrane materials [50].

The core-level spectra of elemental oxygen were shown in Fig. 7. Two main peaks were found in the range 530.5–532.4 eV assigned to carbonyl oxygen [51] and 533.2–534.0 eV assigned to ether oxygen [51]. The increase in the intensity of the first peak and a decrease in the second in the spectra of PEI–BMI–EtOH S and L might be mainly attributed to BMI, which contains higher carbonyl oxygen than PEI and no ether oxygen as seen in Table 3. The presence of amide in PEI–BMI–EtOH S and L might be indicated by the increase in spectrum intensity around 531.5 eV in both membranes [52]. Another possibility for increased peak intensity of carbonyl oxygen and decreased ether oxygen could be additional residual NMP that contains no ether but carbonyl oxygen at a higher concentration than PEI (Table 3).

It was observed that in the spectra of PEI–BMI–EtOH-S membrane, the ether oxygen peak almost disappeared or/and overlapped with the carbonyl oxygen peak, which became more intense than the one in other spectra. This could be explained by the possibility of the shift of ether
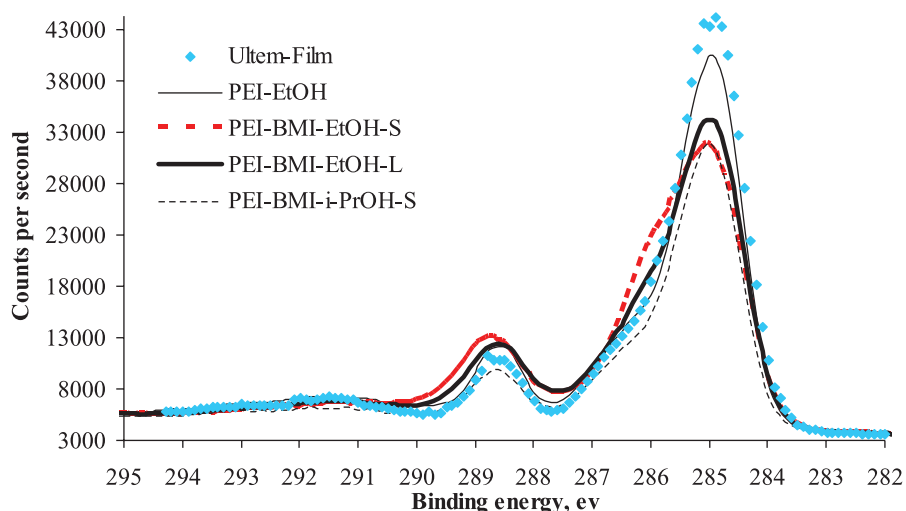

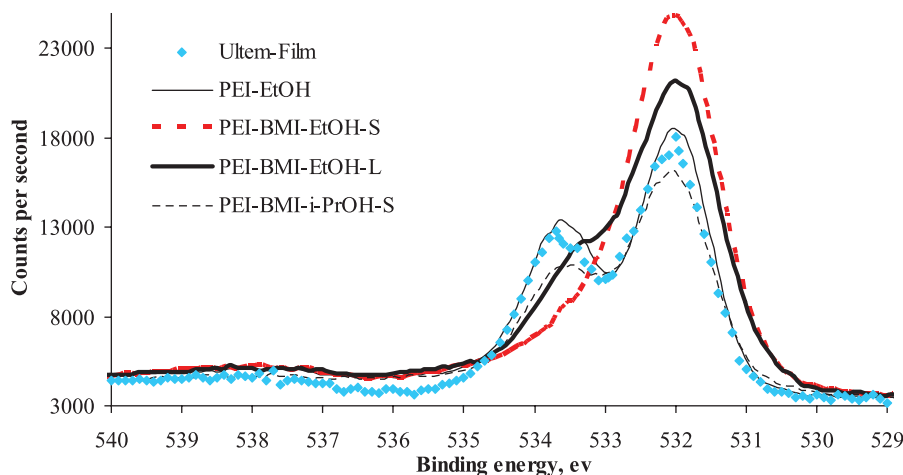Fig. 6. High-resolution XPS core-level spectra of elemental carbon for polyetherimide-based membranes.

Fig. 7. High-resolution XPS core-level spectra of elemental oxygen for polyetherimide-based membranes.

oxygen peak to a lower binding energy due to formation of negative charge on the ether oxygen upon complexation with cationic site or through hydrogen bonding [53,54]. Although, PEI–BMI–EtOH-L and PEI–BMI–EtOH-S were prepared from the same ingredients, the ether oxygen peak appeared again in PEI–BMI–EtOH-L spectra with a decrease in intensity of carbonyl oxygen peak. We might attribute these changes to an increase in time of reactions in which ether groups were incorporated at the expense of carbonyl oxygen. The possibility of ethoxy presence in these membranes as discussed through FTIR results might indicate occurrence of slow ethoxylation reaction with a higher rate in L than in S membranes. The slight decrease in the intensity of carbonyl oxygen peak for the spectra of PEI–BMI–i-PrOH was not clear and might require further study. The broad weak peak around binding energy 538.2 eV was assigned to the oxygen shake up [47]. The decrease in the intensity of this peak for PEI–BMI–i-PrOH and PEI film might be attributed to the lower donor–acceptor charge transfer complexation than other membrane materials [50].

The core-level spectra of elemental nitrogen were shown in Fig. 8. The binding energy in the range of 399.3–400.2 eV was assigned to amide group as reported elsewhere [44,49,55]. The increase in the intensity within this range for PEI–BMI–EtOH (S and L) membranes might be attributed to amide groups resulted from imide cleavage. The binding energy between 400.4 and 401.1 eV was assigned to imide moieties as reported elsewhere [55]. The increase in the intensity of imide peak for PEI–BMI–EtOH (S and L) was attributed to incorporation of BMI that contains higher stoichiometric imide concentration than PEI (Table 3). The complexation with NMP might also lead to an increase in imide concentration for the same reason. The increase in the intensity of PEI–BMI–EtOH S and L spectra at binding energies higher than 401 eV might be explained through many examples found in literature. The H-bonded or positively charged amines have a binding energy at 401.7 eV [55]. An increase in the binding energy from 399.7 to 401.6 eV was observed when amide nitrogen in Nylon-6 was grafted with polyacrylic acid [44]. The presence of electron-withdrawing group such as carbonyl moiety and neighboring amine group lead to an increase in the positive
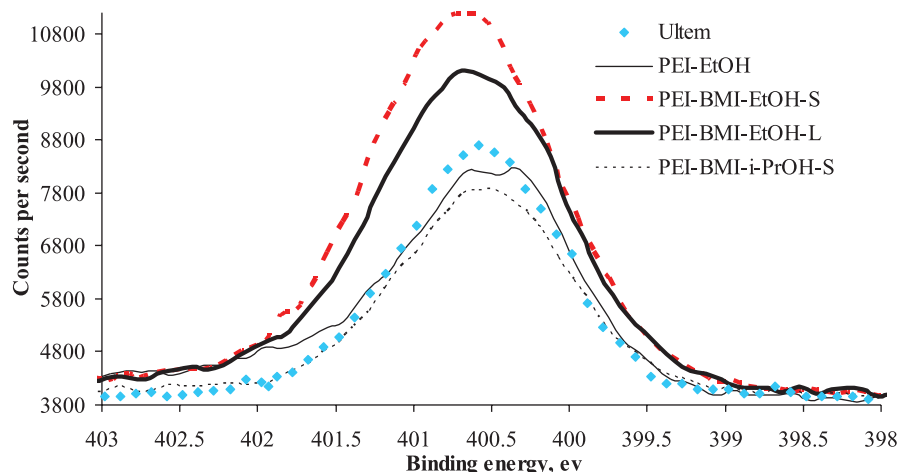

Fig. 8. High-resolution XPS core-level spectra of elemental nitrogen for polyetherimide-based membranes.

charge on nitrogen atom, which results in an increase of BE by 1.0 eV [56]. Therefore, the additional increase in intensity of PEI–BMI–EtOH S and L spectra between 400.7 and 401.7 eV might be attributed to the presence of positively charged nitrogen atoms particularly in amide group that might involve in hydrogen bonding or complexing. The binding energy at 401.7–402.0 eV range was attributed to nitrogen involved in oxidized environment [57]. The BE at 402.3 eV could be assigned to a succinimidyl substituent [58]. Therefore, the increase in the peak intensity for PEI–BMI–EtOH (S and L) within BE between 401.7 and 402.3 eV might indicate membranes containing succinimidyl substituents involved in oxidized environment.

3.2. Gas transport characteristics

The fine morphology including sieving properties of the novel semi-IPNs was analyzed through gas permeation test. Gas permeance and O_2/N_2 selectivity for separation of oxygen from air were shown in Table 5. It was clear that the BMI/PEI semi-IPN prepared using ethanol showed the highest permeance (505 GPU) amongst all structured materials studied. Although permeance was increased by approximately 15 times over the PEI–EtOH membranes, the O_2/N_2 selectivity remained same. The increase in gas permeance could be attributed to the increase in the free volume or pore number in membrane materials or an increase in pore size. Considering that the O_2/N_2 selectivity was not decreased, presence of larger pores was ruled out. Another possibility for increasing gas permeance could be a decrease in the thickness of membrane skin due to different material properties that influence the dynamics of membrane phase inversion. In any case, the high performance suggests that the novel BMI/PEI semi-IPN is a very promising polymeric material suitable for preparation of gas separation membranes.

Comparing the performance of these novel membranes with reported patents, it was clear that at a high O_2/N_2 selectivity of 4.3, the oxygen permeance would usually not exceed 34 GPU [59]. Although we used an old Sylgard 184 silicon rubber coating technique [60], the BMI/PEI semi-

IPN membrane showed air separation performance that was comparable to a recent patent [61], which aimed to develop the coating technique but not the membrane materials. It was also noticed that the gas permeances of the membranes reported elsewhere [61] drop significantly when drying time was increased from 30 to 75 s. It was not clear from this patent if the drying for longer time would change membrane performance or if an additional drying might be required to have stable membranes. The BMI/PEI semi-IPN reported in this work was tested again for air separation after one month and showed the same performance indicating its good stability.

3.3. Formation of the BMI/PEI semi-IPN

Incorporation of BMI into PEI solutions containing i-PrOH as a proton donor in the presence of light leads to a free radical polymerization as shown in Scheme 1 without the need for an initiator (catalyst) or heating to a temperature greater than 180 °C as reported elsewhere [62]. The observed gradual and slow increase in solution viscosity and changing of its color to bright yellow indicated the occurrence of BMI polymerization at ambient temperature.

However, when EtOH was used instead of i-PrOH, the color of polymer solutions was changed to bright red indicating anionic polymerization mechanism. A possible new mechanism for this anionic polymerization under conditions used in this work could be proposed based on the presence of ethoxy group and amic acid (amide + carboxylic) in PEI–BMI–EtOH S and L semi-IPNs as identified by FTIR and XPS in addition to possible occurrence of oxa-Michael addition that is usually accompanied by imide cleavage as illustrated elsewhere [32]. Ethoxy group was substituted in the double bond in one of the maleimide terminal leading to the formation of carbanion (indicated in literature by presence of red color as previously discussed) and proton radicals that may cause initiation and polymerization of BMI as shown in Scheme 2.

As seen in Scheme 2, substituent ethoxy occupies one of the two active sites in the maleimide double bond terminal leading to polymerize this terminal with another maleimide

Table 5
Gas permeance vs O_2/N_2 selectivity for the separation of oxygen from air

Membranes	Total permeance GPU[a]	Oxygen permeance GPU[a]	Selectivity O_2/N_2
PEI–EtOH	33	23	2.3
PEI–i-PrOH	45	31	2.2
PEI–BMI–EtOH-Short	126	87	2.2
PEI–BMI–I-PrOH-Short	130	88	2.1
PEI–BMI–EtOH-Long	505	341	2.1
PEI–BMI–I-PrOH-Long	481	300	1.7
Composite membrane [60]	–	33.2	4.3
Composite membrane dried for 30 s [61]	–	266–826	2.0–2.1
Composite membrane dried for 70 s [61]	–	143–334	2.2–2.3

[a] Gas permeation unit, GPU = 1×10^{-6} (cm^3 (STP)/cm^2 s cmHg).
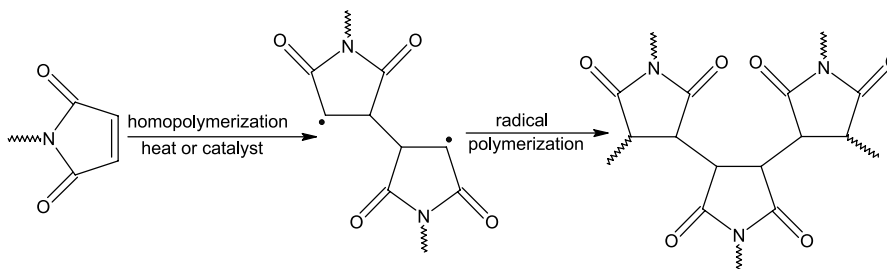
Scheme 1. Radical homopolymerization reaction of BMI, where ⌇⌇⌇ represents the rest of the molecule (BMI in this case).
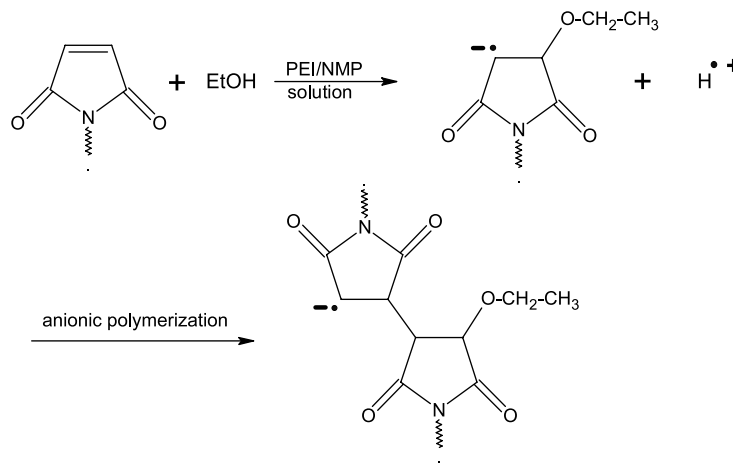
Scheme 2. Ethoxylation reaction, formation of anionic and proton radicals and anionic polymerization of BMI, where ⌇⌇⌇ represents the rest of the molecule.

terminal instead of two terminals as in the case of free radical polymerization of BMI shown in Scheme 1. This might lead to a decrease in the crosslinking density and therefore, PEI–BMI semi-IPN formed by using EtOH might have a lower density structure than the one formed by using i-PrOH. This appears to be plausible as the decrease in the density was consistent with an increase in gas permeation as discussed in Section 3.2. It is worth noting that the combination of many chemical processes such as ethoxylation with in situ polymerization of BMI and imide chemical modification was the reason for formation of new generation of BMI resins that may have lower density structure. This imide chemical modification was indicated by the presence of amic acid, however, as described in literature, the cleavage of imide groups requires an alkaline medium [63] or oxidizing acids such as chromic acid and perchloric acid [64] or catalyst such as Amano PS [65]. As XPS results

indicate the formation of positive charges on imide nitrogen particularly in PEI–BMI–EtOH-S membranes might suggest that the free proton or proton radical produced after ethoxylation process was responsible for imide cleavage in PEI–BMI–EtOH-S and L membranes. The protonation of imide nitrogen weakens the imide-carbonyl bond and therefore, its subsequent cleavage. Further it appears that NMP might be complexed to the PEI–BMI–EtOH S and L membranes. The complexation or substitution of NMP into the new structure might be similar to NMP complexation with polyamic acids as discussed elsewhere [37]. Based on this discussion, we suggest that imide cleavage and NMP complexation could be occurring for imide group and reactions might be illustrated as shown in Scheme 3.

It should be noted that the above two simple reactions are not the only possible reactions within such complex
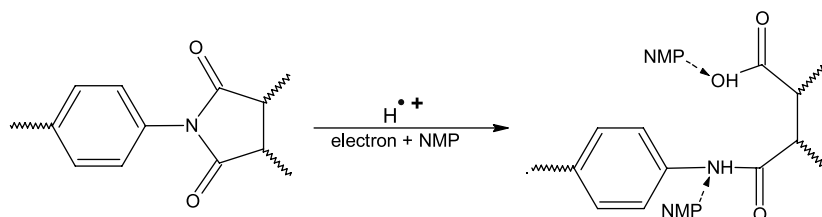
Scheme 3. Imide cleavage that leads to formation of amic acid and then complexation with NMP, where ⌇⌇⌇ represents the rest of the molecule.

BMI/PEI systems. The presence of two domain phases within submicron scale might represent more complex structure of composite materials. Aging, drying and annealing conditions might also influence the amount and presence of various complexes in such composite structure.

4. Conclusions

It was concluded that BMI could be polymerized at ambient conditions in the presence of PEI/NMP and a proton donor without an initiator or catalyst. It was shown that polymerization of BMI in PEI/NMP in the presence of i-PrOH, might have happened through free radical polymerization without imide cleavage. However, replacing i-PrOH by EtOH, imide cleavage and oxa-Michael ethoxylation might have occurred as indicated by FTIR and XPS spectra. It was possible that oxa-Michael ethoxylation of one terminal maleimide group prevented polymerization with two other maleimide terminals leading to a decrease in material density and improved membrane gas permeation. It was shown that the phase separation and stage of termination of BMI polymerization are the keys to produce semi-IPN structures suitable for gas separation membranes. The PEI–BMI–EtOH-L prepared in this work had 15 times higher permeance than membranes prepared from pure PEI without any significant decrease in the selectivity for separation of oxygen from air.

Acknowledgements

References

[1] Mahajan R, Burns R, Schaeffer M, Koros WJ. J Appl Polym Sci 2002; 86(4):881–90.
[2] Baker WR. Ind Eng Chem Res 2002;41(6):1393–411.
[3] Sperling LH, Mishra V. Polym Adv Technol 1996;7:197–208.
[4] Mison P, Sillion B. Adv Polym Sci 1999;140:137–79.
[5] Sperling LH. Interpenetrating polymer networks: An overview. In: Klempner D, Sperling LH, Utracki LA, editors. Interpenetrating polymer networks. Advances in chemistry series, vol. 239, 1994. p. 3–38.
[6] Lee DS, An JH, Kim SC. Adv Chem Ser 1994;239:463–85.
[7] Jackson CL, Bauer BJ, Nakatani AI, Barnes JD. Chem Mater 1996; 8(3):727–33.
[8] Gaina V, Gaina C, Stoleriu A, Timpu D, Sava M, Rusu M. Polym Plast Technol Eng 1999;38(5):927–38.
[9] Kapantaidakis GC, Kaldis SP, Sakellaropoulos GP, Chiran E, Loppinet B, Floudas G. J Polym Sci, Part B: Polym Phys 1999; 37(19):2788–98.
[10] Giannotti MI, Solsona MS, Galante MJ, Oyanguren PA. J Appl Polym Sci 2003;89(2):405–12.
[11] Liou H-C, Ho PS, Tung B. J Appl Polym Sci 1998;70(2):261–72.
[12] Zhang H, Anazawa T, Watanabe Y, Miyajima M, Sommerfeld EG. US patent 6,319,404; 2001.
[13] Koros WJ, Ma YH, Shimidzu T. Pure Appl Chem 1996;68(7): 1479–89.
[14] Dwyer DS, Bradley RJ. Cell Mol Life Sci 2000;57:265–75.
[15] Griesbeck AG, Kramer W, Oelgemöller M. Synlett 1999;(7):1169–78.
[16] Aykurt M, Küçük I, Kuyulu A. Polym Bull 2000;44(3):325–30.
[17] Wang D, Li K, Teo WK. J Membr Sci 1995;98(3):233–40.
[18] Bonnet A, Pascault JP, Sautereau H, Camberun Y. Macromolecules 1999;32(25):8524–30.
[19] Bonnet A, Pascault JP, Sautereau H, Taha M, Camberun Y. Macromolecules 1999;32(25):8517–23.
[20] Stezenberger HD. Adv Polym Sci 1994;117:165–220.
[21] Wang X, Chen D, Ma W, Yang X, Lu L. J Appl Polym Sci 1999;71(4): 665–9.
[22] Tawney PO, Snyder RH, Conger RP, Leibbrand KA, Stiteler CH, Williams AR. J Org Chem 1961;26(1):15–21.
[23] Rozenberg BA, Dzhavadyan EA, Morgan R, Shin E. Polym Adv Technol 2002;13(10–12):837–44.
[24] Chiefari J, Dao B, Groth AM, Hodgkin JH. High Perform Polym 2003;15(3):269–79.
[25] Silverstein RM, Webster FX. Spectrometric identification of organic compounds. 6th ed. New York: Wiley; 1998. p. 71–143 [chapter 3].
[26] Major JS, Blanchard GJ. Chem Mater 2002;14(6):2567–73.
[27] Bajdor K, Glice MM, Les' A, Adamowicz L, Kołos R. J Mol Struct 1999;511–512:107–16.
[28] Shim SC, Bong P-H, Kim JM. Bull Korean Chem Soc 1982;3(4): 153–7.
[29] Sonntag JV, Knolle W, Naumov S, Mehnert R. Chem Eur J 2002; 8(18):4199–209.
[30] Stathatos E, Lianos P, Stangar UL, Orel B. Adv Mater 2002;14(5): 354–7.
[31] Pramoda KP, Liu SL, Chung TS. Macromol Mater Eng 2002;287(12): 931–7.
[32] Mhaske SB, Argade NP. Synthesis. J Synth Org Chem 2003;(6): 863–70.
[33] Seckin T, Koytepe S, Ozdemir I, Çetinkaya B. J Inorg Organomet Polym 2003;13(1):9–20.
[34] de Kok MM, van Breemen AJJM, Carleer RAA, Adriaensens PJ, Gelan JM, Vanderzande DJ. Acta Polym 1999;50(1):28–34.
[35] del Arco M, Carriazo D, Gutiérrez S, Martín C, Rives V. Phys Chem, Chem Phys 2004;6(2):465–70.
[36] Cárdenas G, Acuña J. Colloid J Polym Sci 2001;279(5):442–8.
[37] Shin TJ, Ree M. Macromol Chem Phys 2002;203(5–6):791–800.
[38] Wu W, Wang D, Ye C. Polym Bull 1998;41(4):401–8.
[39] Lin BP, Pan Y, Qian Y, Yuan CW. J Appl Polym Sci 2004;94(6): 2363–7.
[40] Smith B. Infrared spectral interpretation, a systematic approach. Boca Raton: CRC Press; 1999.
[41] Xiao SJ, Brunner S, Wieland M. J Phys Chem B 2004;108(42): 16508–17.
[42] Pompeo F, Resasco DE. Nano Lett 2002;2:369–73.
[43] Mathakiya I, Rakshit AK. J Appl Polym Sci 1998;68(1):91–102.
[44] Liu M, Zhao Q, Wang Y, Niu J, Cao S. Polym Adv Technol 2004; 15(1–2):105–10.
[45] Musto P, Karasz FE, Macknight WJ. Polymer 1989;30(6):1012–21.
[46] Thomas RR, Buchwalter SL, Buchwalter LP, Chao TH. Macromolecules 1992;25(18):4559–68.
[47] Burrell MC, Chera JJ. Surf Sci Spectra 1999;6(1):18–22.
[48] Bubert H, Lambert J, Burba P. Fresenius J Anal Chem 2000;368(2–3): 274–80.
[49] Wolan JT, Hoflund GB. J Vac Sci Technol A 1999;17(2):662–4.
[50] Ågren H, Carravetta V. Int J Quantum Chem 1992;42(4):685–718.
[51] Lin Z, Strother T, Cai W, Cao X, Smith LM, Hamers RJ. Langmuir 2002;18(3):788–96.
[52] Ariza MJ, Rodríguez-Castellón E, Rico R, Benavente J, Muñoz M, Oleinikova M. Surf Interface Anal 2000;30(1):430–3.

[53] Lindberg B, Berndtsson A, Nilsson R, Nyholm R, Exner O. Acta Chem Scand, A: Phys Inorg Chem 1978;32(4):353–9.

[54] Du M, Opila RL, Case C. J Vac Sci Technol, A: Vac Surf Films 1998; 16(1):55–162.

[55] Vinnichenko M, Chevolleau T, Pham MT, Poperenko L, Maitz MF. Appl Surf Sci 2002;201(1–4):41–50.

[56] Ren S, Yang S, Zhao Y, Yu T, Xiao X. Surf Sci 2003;546(2–3):64–74.

[57] Porte'-Durrieu MC, Labruge're C, Villars F, Lefebvre F, Dutoya S, Guette A, et al. J Biomed Mater Res 1999;46(3):368–75.

[58] Jérôme C, Gabriel S, Voccia S, Detrembleur C, Ignatova M, Gouttebaron R, et al. Chem Commun 2003;19:2500–1.

[59] Ding Y, Bikson B, Nelson JK. US patent 6,790,263; 2004.

[60] Henis JMS, Tripodi MK. US patent 4,230,463; 1980.

[61] Nelson JK, Bikson B, Macheras JT. US patent 6,540,813; 2003.

[62] Torrecillas R, Baudry A, Dufay J, Mortaigne B. Polym Degrad Stab 1996;54(2–3):267–74.

[63] Huang XD, Bhangale SM, Moran PM, Yakovlev NL, Pan J. Polym Int 2003;52(7):1064–9.

[64] Ghosh I, Konar J, Bhowmick AK. J Adhes Sci Technol 1997;11(6): 877–93.

[65] Easwar S, Argade NP. Indian J Chem, B: Org Chem Med Chem 2002; 41B(9):1899–902.